HELICON PLASMA SOURCE CONFIGURATION ANALYSIS BY MEANS OF DENSITY MEASUREMENTS*

R.H.Goulding , D.Pavarin[1], F.Angrilli[1],G.C.Barber, M.D.Carter, R.Maggiora[2], D.O.Sparks

Oak Ridge National Laboratory
P. O. Box 2009
Oak Ridge, TN 37831-8071

[1]Center of Studies and Activities for Space (CISAS)
Mechanical Department of Padua University
Via Venezia 1
35131 Padova Italy

[2]Dipartimento di Elettronica
Politecnico di Torino
10129 Torino, Italy

Abstract **Initial results have been obtained from operation of a helicon plasma source built to conduct optimization studies for space propulsion applications. The source features an easily reconfigurable antenna to test different geometries. Operating with He as the source gas, peak densities ≥ 1.6×10^{19} m^{-3} have been achieved. Radial and axial plasma profiles have been obtained using a microwave interferometer that can be scanned axially and a Langmuir probe. The source will be used to investigate operation at high magnetic field, frequency, and input power.**

I. INTRODUCTION

In this paper we report on initial operation of a helicon source built at ORNL for optimization studies geared to space propulsion applications. The specific application for the helicon source at present is to produce plasma for the Variable Specific Impulse Magnetoplasma Rocket (VASIMR)[1], currently under development at the Johnson Space Center in Houston, Texas. The specific research areas being addressed with the ORNL source are: operation with low mass ions (He^+ and H^+), operation at high magnetic field (≤ 0.4 T), frequency (≤ 50 MHz), and power (≤ 3 kW), a comparison of helicon antenna geometries using a special reconfigurable antenna, and optimization of the source configuration. The primary goal is to maximize the fueling efficiency (ions out / neutrals in).

The VASIMR consists of a helicon source followed by an ion heating section in which ion cyclotron resonant heating (ICRH) is used to increase the energy of the ions in the direction perpendicular to the confining magnetic field. The ions then pass through a magnetic nozzle where the perpendicular energy is converted into parallel energy as the magnetic field strength magnitude $|B|$ drops. This produces an exhaust with a very high exit velocity, requiring less mass flow to produce a given change in momentum. Maximizing the fueling efficiency of the helicon source further minimizes the amount of fuel required, as well as reducing charge exchange power losses in the ICRH section.

II. EXPERIMENTAL SETUP

A schematic of the ORNL helicon test chamber is shown in Fig. 1. The magnetic field for the source is generated by a solenoidal magnet which is 48 cm long and has a 14 cm bore. The plasma is produced in a 75 cm long quartz tube with a 5 cm inner diameter which is centered in the magnet bore. Gas is introduced through a metal flange with an o-ring vacuum seal located at one end of the tube. The other end is connected to a larger stainless steel vacuum chamber on which is mounted an additional magnet coil. On the far end of the chamber, a turbo-pump maintains a base vacuum pressure of ~ 2.5_10^{-5} Pa. Radiofrequency (rf) power is coupled into the plasma using an antenna fabricated from 1cm wide copper strips which is located directly outside the quartz tube and fed by a coaxial line. A copper cylinder fitted to the inside of the magnet bore serves as a ground plane and current return path. The antenna is presently configured as a half-turn helix, but is designed so that it

*Oak Ridge National Laboratory, managed by Lockheed Martin Energy Research Corp. for the U.S. department of Energy under contract number DE-AC05-96OR22464.

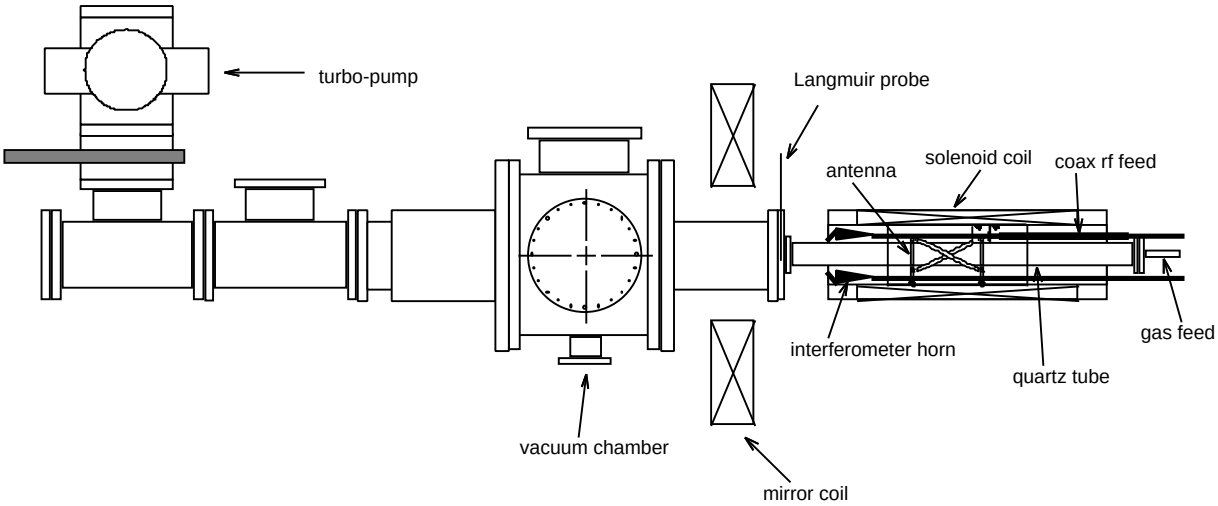

Figure 1. Helicon source test chamber configuration

can easily be converted into a Nagoya type III, or two phased dual half-turn antennas (fig. 2).

The diagnostics currently in use are a radially movable Langmuir probe located between the source and the stainless steel chamber, and a 70 GHz interferometer which can be scanned axially along the quartz source tube (fig. 1). The interferometer features horns parallel to the source tube, with angled reflectors at the ends to produce a beam with O-mode polarization passing through the tube. The waveguide connecting the horns to the measurement leg is arranged to provide sufficient flexibility to allow axial scanning over a range of 30 cm. The remainder of the source tube (except for the region directly under the antenna) can be scanned by removing two short waveguide sections. In addition to these diagnostics, a capacitance manometer is mounted in the gas feed line before the inlet to the source tube to provide an indication of the neutral pressure.

III. INITIAL RESULTS

All of the initial data has been obtained using He gas to produce the plasma, with an rf heating frequency of 13.56 MHz. The device is usually run in a pulsed mode in which gas is puffed into the source tube through a piezoelectric valve, and rf power is then applied to the antenna to form a plasma.

Data from a typical pulse is shown in fig. 3. In this case, the input power is ~1000 W, the neutral pressure in the feed line is 25 Pa at the time of maximum plasma density, and the magnetic field strength in the source regions is ~ 0.16 T. It can be seen that an initial period of constant density is followed by a rapid increase in density. The estimate of ion density n_i was obtained by biasing the probe shown schematically in fig. 1 at –80 V to measure ion saturation current, and using the formula:

$$I_{sat} = 0.6\, A n_i e \sqrt{\frac{kT_e}{M}} \qquad (1)$$

where A is the probe area, e is the charge on an electron, and M is the ion mass. An electron temperature of T_e = 5 eV is assumed. No correction is made to take into account the effect of the background magnetic field. The probe measurement could not be normalized against the interferometer density

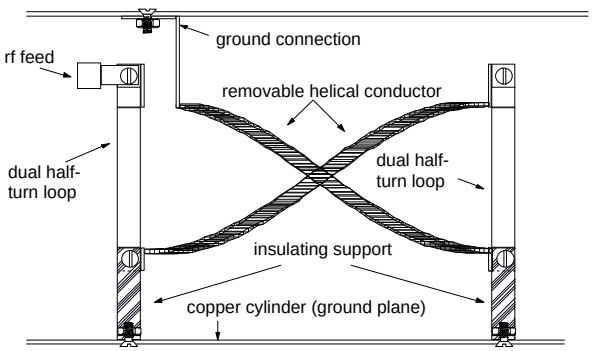

Figure 2. Configurable helicon antenna

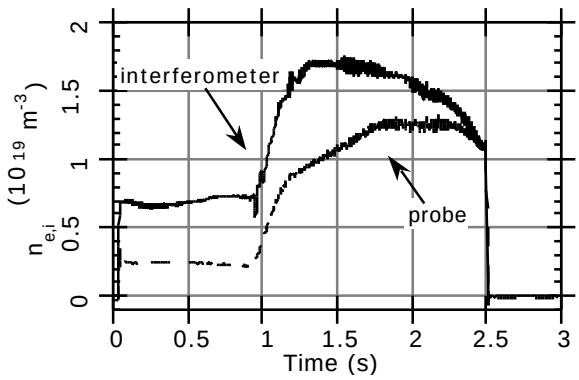

Figure 3. Typical pulse

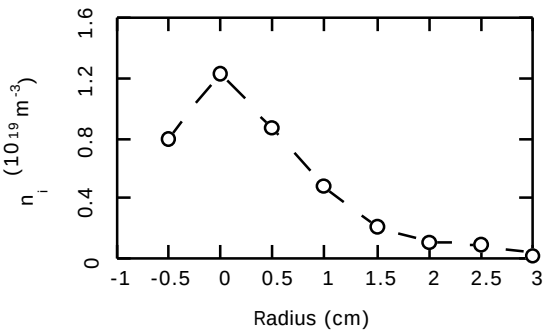

Figure 4. Radial n_i profile from Langmuir probe

measurement because the two measurements could not be made at the same axial location. The "interferometer" curve in fig. 3 is the electron density on axis, calculated using the interferometer line density measurement and the ion saturation current profile from a radial Langmuir probe scan (fig. 4). In calculating the peak (on-axis) density, it was assumed that the ion saturation current profile at the axial location of the probe and interferometer are the same except for changes in the magnetic flux tube size, and that the electron temperature profile is flat in the radial direction.

From fig. 3, it can be seen that the ratio of the apparent density calculated from the Langmuir probe to the density calculated with the interferometer is decreasing throughout the pulse. This is most likely due to an increase in electron temperature throughout the pulse, with a jump at t~1s. The T_e increase is due to a decrease in neutral pressure during the pulse. Dependencies of n_e and T_e on neutral pressure are discussed later in the paper.

Figure 5. shows an axial profile of the peak electron density obtained from an interferometer scan. The scan shows an increase in density as the distance to the antenna decreases. The extent of the scan was limited due to phase errors caused microwaves reflecting off the copper cylinder surrounding the antenna. These errors were large close to the antenna, where presumably the density is higher and diffraction greater. In the future, a microwave

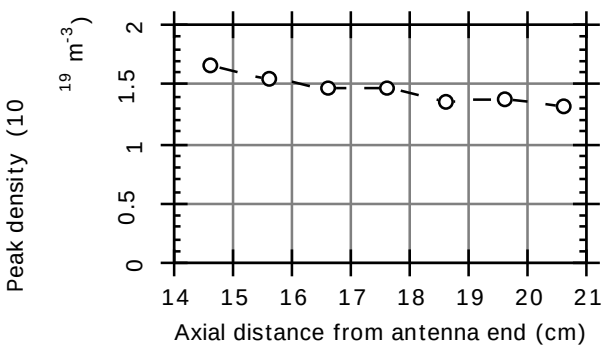

Figure 5. Axial density profile

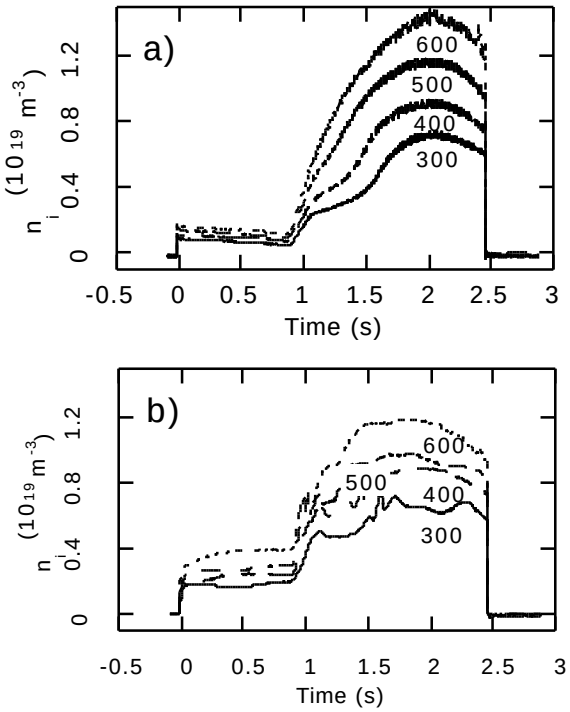

Figure 6. Density determined by a) probe and b) interferometer as a function of I_m, which is indicated by the numbers under the curves (current in Amps).

absorbing material will be placed on the inside of the cylinder to reduce these errors.

The dependence of the measured plasma density on the mirror coil current I_m is shown in figs. 6a and 6b. The ratio of the density calculated with the Langmuir probe to that calculated with the interferometer is seen to increase with increasing I_m. This result, along with the overall increase in density with I_m seen on both diagnostics illustrates the importance of taking into account flux tube mapping in interpreting source behavior based on results from "downstream" diagnostics. The reasoning is as follows: Figure 7 shows the effect of the change in I_m on a flux tube referenced to a particular radius (1.08 cm) in the source, chosen because it just intercepts the quartz

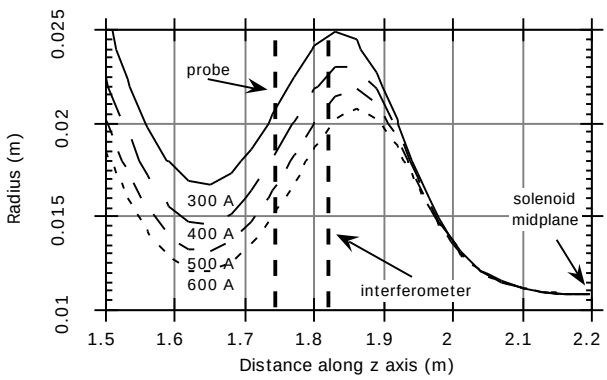

Figure 7. Magnetic flux tube mapping for different mirror coil currents referenced to r=0.0115 m at the solenoid midplane

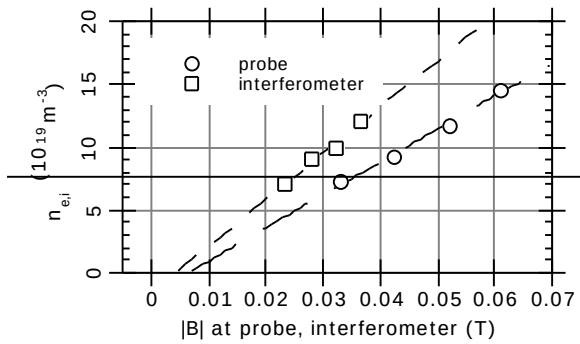

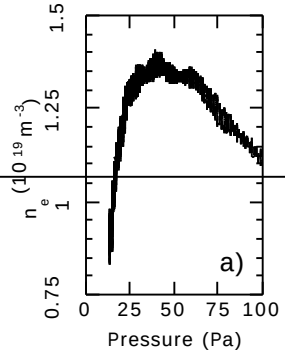

Figure 8. Density dependence on |***B***| on axis at axial location of diagnostics.

tube (at r=2.5 cm) at the lowest mirror coil current of 300 A. It can be seen from the figure that the relative radial compression of the magnetic flux as a function of mirror coil current is higher at the probe location than at the interferometer location. From fig. 8, it can be seen that the density measured by both diagnostics (assuming constant T_e for the probe) scales linearly with $|B|$. A simple interpretation of this behavior and the greater increase in density with I_m observed with the probe relative to the interferometer is as follows: The plasma parameters in the solenoid region do not vary with I_m because $|B|$ remains constant there. A constant ion flux at constant velocity flows from this region, causing the plasma density in a given flux tube to be inversely proportional to the flux tube area, or proportional to $|B|$, as is indeed seen (fig. 8). The density increases faster with I_m at the probe than at the interferometer because the relative flux tube compression is greater at the location of the former.

The actual behavior is more complicated than this picture of a constant ion flux at constant velocity, due partly to the high neutral-ion collision frequency. In fact, the plasma density is observed to decrease away from the source (fig. 5), in a region around the magnetic field minimum where $|B|$ is nearly constant. Still, the large variations seen in fig.6 with I_m can be qualitatively explained in this way. Another objection is that the high neutral pressure and resulting high ion-neutral collision frequency should greatly reduce the effects of the magnetic field changes caused by the mirror coil. However, this is clearly not the case. An absence of degradation of magnetic confinement in helicon sources due to increasing ion-neutral collisions as the fill pressure is raised has also been observed by other experimenters[2].

Figure 9 shows the dependence of the plasma density and electron temperature on axis on the neutral pressure. The data was obtained during a single pulse. The electron temperature shown is an estimate obtained from eqn (1) with n_i taken from interferometer data (assuming n_e=n_i) and I_{sat} from the Langmuir probe. It should be interpreted qualitatively since the two diagnostics are at differing axial locations. The results are similar to those seen in inductive, unmagnetized plasma sources[3]. The fact that a maximum is seen in the electron density n_e as the pressure is scanned may indicate that the power loss channels associated with ionization and excitation are more important than those associated with particle loss [3]. This is not usually seen with monatomic gasses, but may be due to the additional confinement provided by the magnetic field. We have begun a modeling effort in an attempt to better understand the source behavior.

CONCLUSIONS

Operation of a helicon plasma source to be used to determine the optimum configuration of a source for a VASIMR space propulsion system has begun. Good initial performance using He gas has been obtained, with peak plasma densities $\geq 1.6\times10^{19}$ m^{-3} observed with ~1kW input power. At the present time density diagnostics are only available in the exhaust region of the source, and density in this region has been found to depend linearly on the value of |B| there. Future work will include operation at higher values of |B| in the source region, operation with different antenna configurations and locations, and operation using hydrogen gas. In addition, a modeling effort has begun to understand the relation of plasma parameters to device inputs.

REFERENCES

[1] F.R. Chang Díaz, “Research Status of the Variable Specific Impulse Magnetoplasma Rocket”, *Transactions of Fusion Technology*, Vol. 35, Jan. 1999, pp. 87-93.

[2] A. D. Cheetham and J. P. Rayner, J. Vac. Sci. Technol. A. **16**, Sept/Oct 1998, p. 2777.

[3] C. Lee and M. A. Lieberman, J. Vac. Sci. Technol. A. **13**, Mar/Apr 1995, p. 368.